

Supplemental Material: Violations of Jeffery’s theory in the dynamics of nanographene in shear flow

Simon Gravelle and Catherine Kamal

School of Engineering and Material Science, Queen Mary University of London, London, United Kingdom

Lorenzo Botto*

*Process and Energy Department, 3ME Faculty of Mechanical,
Maritime and Materials Engineering, TU Delft, Delft, The Netherlands*

Simulations details. MD simulations were performed using LAMMPS [1]. The TIP4P/2005 model was used for water [2], and the water molecules were kept rigid with the SHAKE algorithm [3]. The all atom Gromos force field was used for the (unmodified) aromatic molecules, as well as for N-Methyl-2-pyrrolidone (NMP) molecules [4]. Long-range Coulombic interactions were computed using the particle-particle particle-mesh (PPPM) method [5, 6]. Initial aromatic and NMP molecular structures were extracted from the automated topology builder [7]. Following Ref. 8, the LJ parameters of the rigid walls with a close-packed density of $\rho_w = \sigma_{ww}^{-3}$ were $\sigma_{ww} = 3.374 \text{ \AA}$ and $\epsilon_{ww} = 2.084 \text{ kcal/mol}$. Crossed parameters (σ_{ij} and ϵ_{ij}) were calculated using the Lorentz-Berthelot mixing rule: $\sigma_{ij} = (\sigma_{ii} + \sigma_{jj})/2$ and $\epsilon_{ij} = \sqrt{\epsilon_{ii}\epsilon_{jj}}$.

In order to differentiate between the solvent molecules (water and NMP) and the solute molecules (aromatic molecules), we sometimes refer to the solute molecules as ‘particles’.

No-slip HBC. In order to model aromatic molecules in water solvent with the no-slip boundary condition, the value of the LJ parameter ϵ_{CO} , where the ‘C’ stands for the carbon atoms of the aromatic molecules, and the ‘O’ stands for the oxygen atoms of the water molecules, was increased. The slip length λ was measured for varying values of ϵ_{CO} , from $\epsilon_{CO} = 0.35$ to 1.4 kcal/mol , using Poiseuille flow simulations of a liquid confined between two planar graphene walls. In short, the position where the slip boundary condition applies is determined from the Gibbs dividing plane, and the slip length is extracted from a fit of the velocity profile in the bulk region, see Ref. [9] for details. Slip length values for varying values of ϵ_{CO} are given in Table I. The value of $\epsilon_{CO} = 1.4 \text{ kcal/mol}$ was chosen to ensure $\lambda < b$, where $b \approx 2.5 \text{ \AA}$ is the half thickness of an aromatic molecule.

Single-particle dynamics simulations. Single-particle dynamics simulations were carried out using a single aromatic molecule immersed in either water or NMP. The solution (aromatic molecule + solvent) was enclosed in the \vec{e}_y direction by two rigid walls, and a linear shear flow of strength $\dot{\gamma}$ was produced by the relative translation of these walls (see Fig. 1 of the main text). The two walls separated by a distance $H \approx 6 \text{ nm}$, were also used to impose $p = 1 \text{ atm}$ as ambient pres-

sure. The solvent was made of $N_s = 3000$ molecules in the case of $C_{42}H_{18}$ in water, $N_s = 8000$ molecules in the case of $C_{114}H_{30}$ in water, and $N_s = 336$ molecules in the case of $C_{42}H_{18}$ in NMP. The aromatic molecule was free to rotate and translate. Unless explicitly stated, the molecule was also free to deform. The box had lateral dimensions $L_x = L_z = 3 \text{ nm}$ in the case of $C_{42}H_{18}$, and $L_x = L_z = 5 \text{ nm}$ in the case of $C_{114}H_{30}$. Periodic boundary conditions were used along the three orthogonal directions. A temperature $T = 300 \text{ K}$ was maintained using a Berendsen thermostat applied only to the solvent, and only to the degree of freedom perpendicular to the direction of the flow. Data were recorded after an equilibrium step of duration 1 ns .

Multiple-particle dynamics. Multiple-particle simulations are identical to single molecule dynamics simulations, expect for the number of solute molecules. Solute molecules were initially randomly distributed, and data were recorded after an equilibrium step of duration 10 ns .

Data acquisition. For each situation, a number N of independent simulations is performed, with N varying from 5 (in the case of a high Péclet number) to 30 (in the case of a low Péclet number). Error bars can be calculated from the standard deviation, see Figs. S4 and S5.

Lees-Edwards boundary conditions. When specified, Lees-Edwards boundary conditions [10] were used to realize a sheared system without bounding walls. With these boundary conditions, a shear is provided by giving each periodic domain a velocity proportional to the domain’s vertical position compared to the center domain ($u_{LE} = \dot{\gamma}L_y$). The size of the system was $L_x = L_z = 3 \text{ nm}$ and $L_y = 6 \text{ nm}$. The fluid was made of $N_s = 3000$ water molecules and $N = 16$ HBC molecules, and the shear rate was $\dot{\gamma} = 100 \text{ ns}^{-1}$.

Rotational diffusion coefficient measurement. The rotational diffusion coefficient D_r for $C_{42}H_{18}$ and $C_{114}H_{30}$ was calculated from autocorrelation function analysis [11, 12]. The simulation consisted of a cubic box containing a single aromatic molecule immersed in the solvent water or NMP. The solute molecule was free to rotate and deform, and was maintained in the center of the box. The vector \mathbf{n} , defined as the normal to the surface at the center of the molecule, and its autocorrelation function $\langle \mathbf{n}(0)\mathbf{n}(t) \rangle$ was

computed. The data was found to follow an exponential decay

$$\langle \mathbf{n}(0)\mathbf{n}(t) \rangle = e^{-t/\tau}, \quad (\text{S1})$$

where τ is the rotational relaxation time scale. For HBC in water, we find $\tau = (190 \pm 20)$ ps. For HBC in NMP, we find $\tau = (1500 \pm 100)$ ps in NMP. For the $\text{C}_{114}\text{H}_{30}$ molecule in water, we find $\tau = (1000 \pm 300)$ ps. The corresponding rotational diffusion coefficients calculated as $D_r = 1/(6\tau)$ are $D_r = (0.9 \pm 0.1) \text{ ns}^{-1}$, $D_r = (0.1 \pm 0.1) \text{ ns}^{-1}$, and $D_r = (0.16 \pm 0.05) \text{ ns}^{-1}$, respectively. Note that the instantaneous diffusion coefficient of a flexible molecule depends on its instantaneous shape. The reported values are temporal averages.

Effective aspect ratio measurement. The effective aspect ratio k_e of an aromatic molecules was evaluated using Eq. 6 of the main text. The molecule was frozen, and maintained at a fixed angle with respect with the flow, either aligned with the flow ($\varphi = 0, \theta = \pi/2$), either normal to the flow ($\varphi = \pi/2, \theta = \pi/2$). A shear flow $\dot{\gamma} = 10 \text{ ns}^{-1}$ was applied thanks to the moving walls, and the average torque applied by the solvent to the frozen molecule was measured. Then, the effective aspect ratio was deduced following Eq. 6 of the main text. For HBC in water, we find $k_e = 0.41i$, for the $\text{C}_{114}\text{H}_{30}$ molecule in water, we find $k_e = 0.43i$, and for HBC in NMP, we find $k_e = 0.59i$. Imaginary values for k_e are expected when the slip length λ is larger than the half thickness b of the molecule [13]. Additionally, for the no-slip HBC, we find $k_e = 0.43$.

Bending rigidity measurement. The measurement of the bending rigidity of the aromatic molecules was performed in vacuum. Bending rigidity was evaluated from calculations of the strain energy of molecules subjected to a point loading [14, 15]. A point loading was applied at the center of the molecule, while the hydrogen atoms at the edges were maintained clamped. The relationship between the loading F and the deformation at the loading position w is

$$\frac{F}{w} = \frac{B}{\beta(2a)^2}, \quad (\text{S2})$$

where $\beta = 0.0056$ and B is the bending rigidity. We measure $B = 1.1 \text{ eV}$ for the $\text{C}_{42}\text{H}_{18}$ molecule, and $B = 1.2 \text{ eV}$ for the $\text{C}_{114}\text{H}_{30}$ molecule. Consistently with previous observation (see Ref. [14]), the bending rigidity of single layer nanographene depends on its dimension.

ϵ_{CO} (kcal/mol)	λ (nm)
0.35	7.28 ± 2
0.46	2.51 ± 0.5
0.58	1.23 ± 0.2
0.69	1.17 ± 0.2
0.81	0.2 ± 0.1
0.92	< 0.1
1.04	< 0.1
1.15	< 0.1
1.26	< 0.1
1.4	< 0.1

TABLE I. Slip length λ as measured from MD.

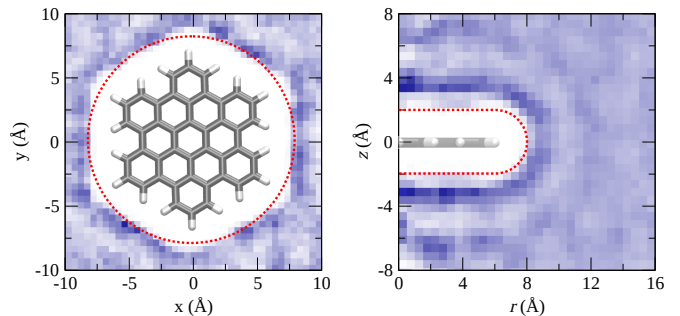


FIG. S1. Water density profile near the HBC, from white (low density) to blue (high density). The radial coordinate r is defined as $r = \sqrt{x^2 + y^2}$, and the normal \mathbf{n} to the center of the HBC is oriented along z . The red dotted lines show the effective shape of the HBC (i.e. the shape as seen by the water molecules).

- [2] J. L. Abascal and C. Vega. A general purpose model for the condensed phases of water: TIP4P/2005. *The Journal of chemical physics*, 123(23):234505, dec 2005.
- [3] Jean-Paul Ryckaert, Giovanni Ciccotti, and Herman J.C Berendsen. Numerical integration of the cartesian equations of motion of a system with constraints: molecular dynamics of n-alkanes. *Journal of Computational Physics*, 23(3):327–341, 1977.

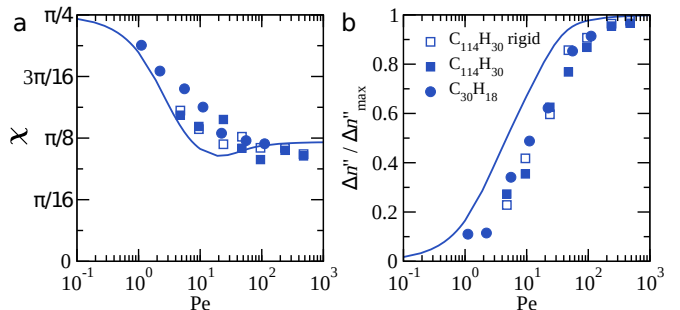


FIG. S2. (a) Average orientation angle χ and (b) degree of alignment $\Delta n''/(\Delta n''_{\text{max}})$ for $N = 1$ and respectively: HBC molecule in water (disks); $\text{C}_{114}\text{H}_{30}$ molecule in water (full squares); rigid $\text{C}_{114}\text{H}_{30}$ molecule in water (open squares). Lines are theory with $k_e = 0.4i$.

* l.botto@tudelft.nl

[1] S Plimpton. Fast Parallel Algorithms For Short-range Molecular-dynamics. *J. Comp. Phys.*, 117(1):1–19, 1995.

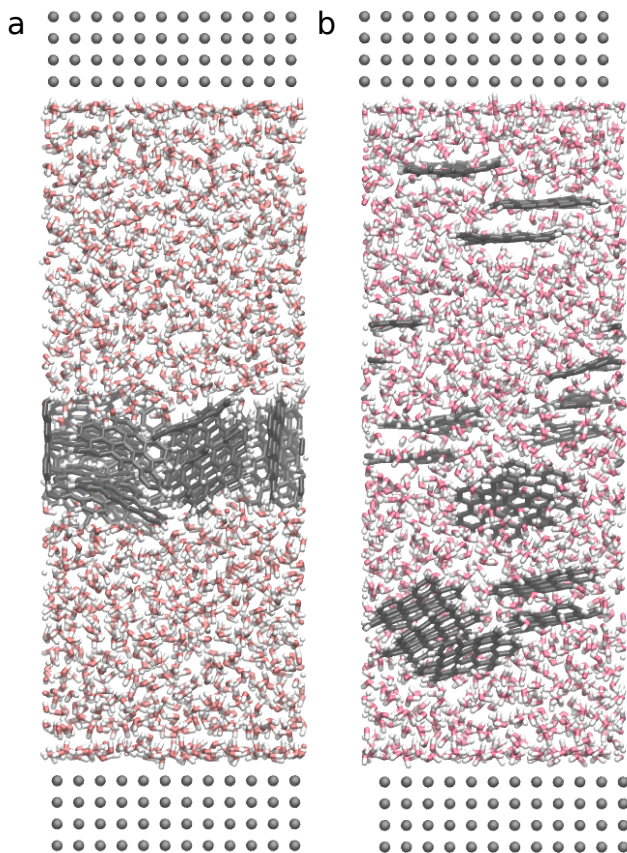


FIG. S3. **Clustering of HBC molecules in water.** (a) $N = 16$ HBC molecule and $Pe = 1.1$. (b) $N = 16$ HBC molecule and $Pe = 62$. HBC molecules are in gray and water molecules in red and white.

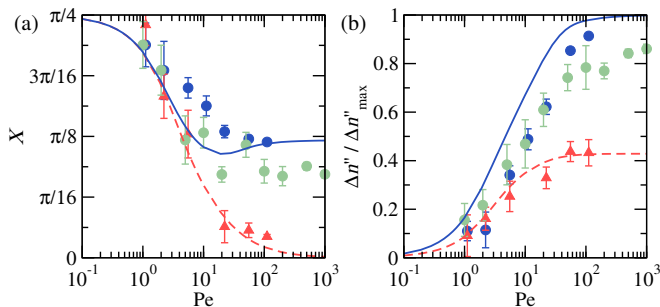


FIG. S4. (a) Average orientation angle χ and (b) degree of alignment $\Delta n'' / (\Delta n''_{\max})$ for $N = 1$: slip HBC in water (blue disks); slip HBC in NMP (green disks); no-slip HBC in water (red triangles). Lines are theory, see the main text for details.

- [4] Nathan Schmid, Andreas P. Eichenberger, Alexandra Choutko, Sereina Riniker, Moritz Winger, Alan E. Mark, and Wilfred F. Van Gunsteren. Definition and testing of the GROMOS force-field versions 54A7 and 54B7. *European Biophysics Journal*, 40(7):843–856, 2011.
- [5] Tom Darden, Darrin York, and Lee Pedersen. Particle mesh Ewald: An $N \log(N)$ method for Ewald sums in large systems. *The Journal of Chemical Physics*, 98(12):10089, 1993.

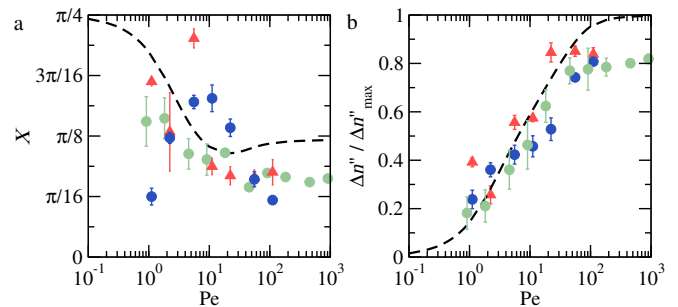


FIG. S5. (a) Average orientation angle χ and (b) degree of alignment $\Delta n'' / \Delta n''_{\max}$ for varying Pe and multiple HBCs ($N = 16$): slip HBCs (blue disks) and no-slip HBCs (red triangles) in water; slip HBCs in NMP (green disks). Dashed lines are the theory for $N = 1$.

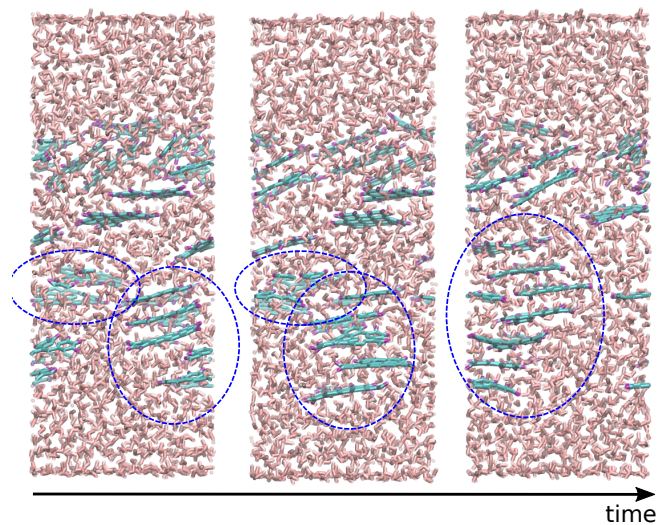


FIG. S6. Snapshots of the molecular dynamics simulation showing a number $N = 16$ HBCs (in cyan) in water for $Pe = 62$. Snapshots are taken at intervals of 10 ps. The dashed blue lines highlight the merging of two clusters made respectively of 2 and 5 HBCs (left and middle images) into a single cluster of 7 HBCs (right image).

- [6] Qiang Lu and Ray Luo. A Poisson-Boltzmann dynamics method with nonperiodic boundary condition. *Journal of Chemical Physics*, 119(21):11035–11047, 2003.
- [7] Alpeshkumar K. Malde, Le Zuo, Matthew Breeze, Martin Stroet, David Poger, Pramod C. Nair, Chris Oostenbrink, and Alan E. Mark. An Automated force field Topology Builder (ATB) and repository: Version 1.0. *Journal of Chemical Theory and Computation*, 7(12):4026–4037, 2011.
- [8] David M. Huang, Cécile Cottin-Bizonne, Christophe Ybert, and Lydéric Bocquet. Aqueous electrolytes near hydrophobic surfaces: Dynamic effects of ion specificity and hydrodynamic slip. *Langmuir*, 24(4):1442–1450, 2008.
- [9] Cecilia Herrero, Takeshi Omori, Yasutaka Yamaguchi, and Laurent Joly. Shear force measurement of the hydrodynamic wall position in molecular dynamics. *Journal of*

- Chemical Physics*, 151(4):041103, 2019.
- [10] A. W. Lees and S. F. Edwards. The computer study of transport processes under extreme conditions. *J. Phys. C*, 5:1921–1929, 1972.
- [11] A. Ortega and J. Garcia De La Torre. Hydrodynamic properties of rodlike and dislike particles in dilute solution. *Journal of Chemical Physics*, 119(18):9914–9919, 2003.
- [12] Ali Kharazmi and Nikolai V. Priezjev. Molecular Dynamics Simulations of the Rotational and Translational Diffusion of a Janus Rod-Shaped Nanoparticle. *Journal of Physical Chemistry B*, 121(29):7133–7139, 2017.
- [13] Catherine Kamal, Simon Gravelle, and Lorenzo Botto. Hydrodynamic slip can align thin nanoplatelets in shear flow. *Nature Communications*, 11:1–10, 2020.
- [14] Q. Wang. Simulations of the bending rigidity of graphene. *Physics Letters, Section A: General, Atomic and Solid State Physics*, 374(9):1180–1183, 2010.
- [15] Vadym N. Borysiuk, Vadym N. Mochalin, and Yury Gogotsi. Bending rigidity of two-dimensional titanium carbide (MXene) nanoribbons: A molecular dynamics study. *Computational Materials Science*, 143:418–424, 2018.